

Article

Use of Sodium Hexametaphosphate and Citric Acid Mixture as Depressant in the Flotation Separation of Scheelite from Calcite

Wenlong Zhu ^{1,2}, Liuyang Dong ^{1,2,*}, Fen Jiao ^{1,2}, Wenqing Qin ^{1,2} and Qian Wei ^{1,2}

¹ School of Minerals Processing and Bioengineering, Central South University, Changsha 410083, China; 13787790983@163.com (W.Z.); jfen0601@126.com (F.J.); qinwenqing369@126.com (W.Q.); weiqianjiayou@163.com (Q.W.)

² Key Laboratory of Hunan Province for Clean and Efficient Utilization of Strategic Calcium-containing Mineral Resources, Central South University, Changsha 410083, China

* Correspondence: 185601031@csu.edu.cn; Tel.: +86-731-88830346

Received: 13 August 2019; Accepted: 12 September 2019; Published: 16 September 2019



Abstract: The floatability of scheelite and calcite in the presence of single depressant (SHMP or H₃Cit) and mixed depressant (SHMP/H₃Cit) was studied by microflotation experiments and artificial mixed mineral experiments. Solution chemical calculation, zeta potential tests, thermodynamic analysis and XPS analysis were used to explain the relevant depressive mechanism. Mixed depressant (SHMP/H₃Cit) exhibited excellent selective depressive effect on calcite. The optimal molar ratio of SHMP to H₃Cit was 1:4. The depressant SHMP and H₃Cit can be chemically bonded with Ca²⁺ to form CaHPO₄ and Ca₃(Cit)₂ at pH 8. The CaHPO₄ was more easily formed than Ca₃(Cit)₂ on the mineral surface, which indicated that the depressive effect of SHMP was stronger than H₃Cit. The SHMP and H₃Cit of the mixed depressant were co-adsorbed on the calcite surface, while the H₃Cit of the mixed depressant was weakly adsorbed on the scheelite surface. The mixed depressant can significantly improve the separation efficiency of scheelite from calcite.

Keywords: scheelite; calcite; mixed depressant; citric acid; sodium hexametaphosphate

1. Introduction

Scheelite and wolframite are the two most important tungsten resources in nature. Since the wolframite ((Fe, Mn)WO₄) is more easily enriched by gravity methods and is easier to exploit and utilize, the wolframite resources have been exhausted [1–3]. Therefore, the exploitation and high standards utilization of scheelite (CaWO₄) are receiving more and more attention [4,5]. The extraction of scheelite from corresponding gangue minerals has been a problem due to its unique embedding characteristics and symbiotic relationship [6]. Foam flotation is an efficient method to recover minerals with low grade and fine grain size [7–9]. During the flotation process, the chemical properties of the mineral surface (such as wettability and surface electrical properties) are changed by adding flotation reagents [10–13]. Similarly, scheelite and calcite have similar chemical compositions and chemical interactions with corresponding flotation reagents, which makes the separation of scheelite and calcium-containing minerals different [14]. Therefore, the flotation of scheelite is also facing enormous challenges in the process of utilization of tungsten resources [15]. Flotation reagents are the key to improving flotation indicators. The most important flotation reagents are mainly collectors [16,17], depressants [18,19] and regulators [20]. The role of the depressants in flotation is mainly to selectively be adsorbed on certain mineral surfaces to reduce their floatability [21,22]. Therefore, increasing the selectivity and the depressive ability of depressants is the focus of scheelite flotation research. As such, the reasonable choice of scheelite flotation depressants is the key to recovering scheelite.

Sodium silicate (water glass) has been widely used as a depressant in flotation of scheelite from calcite [23]. However, sodium silicate also has some disadvantages as a depressant, such as frequent acidification, narrow optimum pH range, and weak selectivity. Single phosphates are also used for calcite depressants, but they are often limited by their weak selectivity, so mixed reagents are often required [24]. Organic macromolecular depressants have also received attention. Zhang et al. studied the role of sodium polyacrylate in flotation separation of scheelite and calcite [25]. However, sodium polyacrylate also has an unfavorable inhibitory effect on scheelite over a wide range of pH conditions, with poor flotation selectivity. Carboxymethyl cellulose has also been studied as a depressant in the flotation separation of scheelite from calcite [26], but it is difficult to dissolve carboxymethyl cellulose at room temperature, which is not conducive to flotation. In view of the shortcomings of the above single depressants, such as poor collecting ability, weak selectivity, and large dosage, it is often necessary to use mixed depressant to achieve flotation separation between scheelite and gangue minerals.

Sodium hexametaphosphate (SHMP) is a clean, non-toxic phosphate that is widely used in the food industry and the chemical industry [27,28]. It can be used as a chelating reagent for metal ions, an adhesive, and a swelling reagent [29,30]. It is also widely used in the mineral processing industry, especially in the flotation. SHMP is used as a dispersant and depressant of minerals in flotation [31–35]. In addition, SHMP can be used to depress calcite [24], but it also has a strong depressive effect on scheelite. Citric acid (H_3Cit) is also a clean, non-toxic organic acid and is a tricarboxylic acid compound. It is mainly used in the food industry, chemical industry, textile industry, cosmetics and pharmaceutical industries [36–38]. Citric acid can be used as depressant in flotation [39–41]. In the dolomite flotation, it can be used to depress apatite [42]. A related study showed that the floatability of rare earth can be inhibited by citric acid [43]. Zeng et al. studied the depression of H_3Cit in the process of separating celestite from fluorite and calcite [44]. It is a pity that they did not study the depression of H_3Cit in the process of separating scheelite from calcite. At the same time, the effect of the mixed depressant SHMP/ H_3Cit on the flotation separation of scheelite from calcite had not been systematically studied. The corresponding depressive mechanism of the depressants remain unclear.

In this study, single depressant SHMP or H_3Cit was studied in the process of separating scheelite from calcite. Sodium oleate (NaOL) was used as a collector during this process. In contrast, mixed depressant SHMP/ H_3Cit was also studied and eventually the best molar ratio was obtained. The floatability of the two minerals under different depressants systems was investigated by microflotation experiment. The flotation separation efficiency of scheelite from calcite was studied by artificial mixed mineral experiments. The depression mechanism of depressant was studied by the solution chemical analysis of the mineral soluble component and the depressant solution. Furthermore, it was proved by the zeta potential of the mineral surfaces. Thermodynamic analysis of the reaction between the depressants and the minerals can characterize the ease with which reaction products are formed. The chemical environment of the elements after the conditioning with corresponding depressant was changed, which can be analyzed by XPS experiment. This can further reveal the adsorption mechanism of the depressants on the mineral surfaces.

2. Material and Methods

2.1. Material

The mineral samples with high purity of scheelite and calcite were from Guangxi and Hunan, China. Blocky pure scheelite and calcite are shown in Figure 1. At the beginning, the samples were hand-selected, and then the large particle size was hammered into a uniform small particle size. Then, it continued to be ground and the particle size of $-74 + 37 \mu m$ was sieved by dry sieves for microflotation experiments. Particle size less than $37 \mu m$ was then further ground to below $5 \mu m$ for the mechanism experiments, chemical analysis and X-ray diffraction analysis (XRD). Chemical analysis showed that the scheelite sample had a purity of 96% and additionally contained 2.12% SiO_2 and 1.75%

MgO, and the calcite sample had a purity of 98.91% and additionally contained 1.01% SiO₂. The XRD also represented extremely high purity (Figure 2).

The depressants SHMP (the content of P₂O₅ is 65.0–70.0%) and H₃Cit (purity greater than 99.5%) with analytical grade used in this experiment were from Tianjin Komiou Chemical Reagent Co., Ltd., China. and Hunan Huihong Reagent Co., Ltd., Changsha, China. respectively. Analytically pure NaOL was also obtained from Hunan Huihong Reagent Co., Ltd., China. Ultrapure water was used in all experiments (resistance over 18 MΩ × cm).

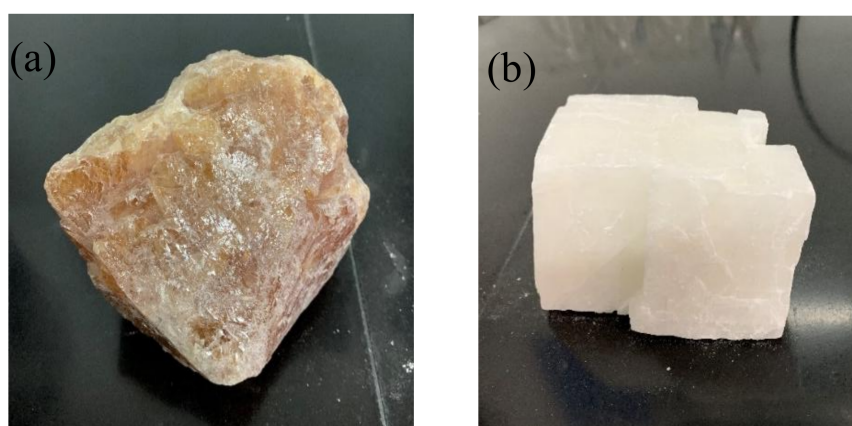


Figure 1. The images of pure scheelite (a) and calcite (b).

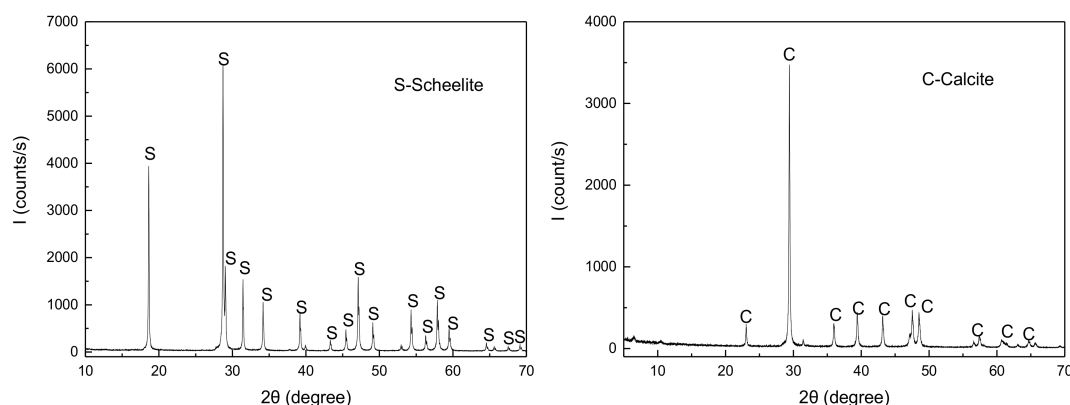


Figure 2. XRD of the two minerals.

2.2. Methods

2.2.1. Microflotation

The floatability of the two minerals in the presence of different reagents was investigated using an XFGC_{II} flotation machine (capacity 40 mL) with a spindle speed 1500 r/min (Figure 3). 35 mL of ultrapure water and 2.0 g of pure mineral were mixed and stirred for 2 min. The pH of the slurry was then adjusted and recorded. The flotation reagents were then added in sequence and the conditioning time was as shown in Figure 4. The flotation time was also 3 min. The flotation recovery was calculated by the following formula:

$$\varepsilon = \frac{m_1}{m_1 + m_2} \times 100\%$$

In the formula, m_1 and m_2 represent the floated products weight and sunk products weight, respectively. Microflotation experiments under the same conditions were repeated three times, and the average value was reported in the flotation results. The standard deviation for each test was calculated and presented as the error bars.

For the artificial mixed mineral tests, 1 g of scheelite and 1 g of calcite were mixed into mixed minerals. After the mixed minerals were stirred for 1 min, the flotation reagents were added. The foam product was collected as the concentrate product, and the sinked product was the tailing. The concentrate product and tailing product were weighed separately and the yields were calculated. The flotation recovery was calculated based on the yields and the scheelite grade of the two products.



Figure 3. The image of microflotation machine (XFGC_{II}, Jilin Exploration Machinery Plant, Changchun, China).

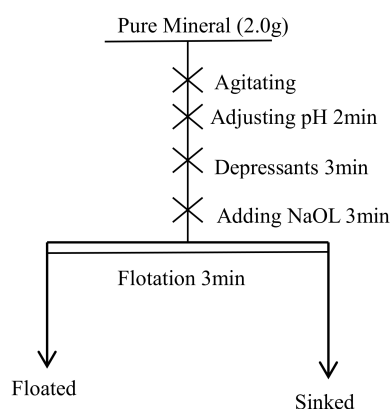


Figure 4. Schematic diagram of pure mineral microflotation process.

2.2.2. Zeta Potential Analysis

Zeta potential analysis was performed using a zeta potential analyzer. The device model is ZetaPlus and the device manufacturer is Bruker, Karlsruhe, Germany. First, 30 mg of samples ($-5 \mu\text{m}$) and 35 mL of KNO_3 electrolyte solution were added to a beaker and stirred with a magnetic stirrer to bring the slurry in suspension. Then, corresponding flotation reagents were added, and the dosages of the reagents and the conditioning time were consistent with the microflotation experiment. The conditioning time of each flotation reagent was 3 min. After the conditioning, the slurry suspension was allowed to stand for 5 min, and the supernatant was withdrawn by a syringe for testing. Under each condition, the value was tested three times to obtain an average value. The standard deviation for each test was calculated and presented as the error bars.

2.2.3. XPS Analysis

In this experiment, XPS analysis was performed using an X-ray photoelectron spectrometer. The device model is ESCALAB 250Xi and the device manufacturer is Thermo Fisher, Waltham, MA, USA. X-ray source is monochromatic Al K α X-ray source operating at 150 W. The fitting of the peaks was performed using the XPS PEAK fitting software (Version 4.1). The preparation process of the samples used for XPS analysis was consistent with the microflotation experiments. The samples were contaminated with hydrocarbons in an open system, so carbon can be detected on the surface of pure scheelite. The chemical state of the elements (such as binding energy, etc.) was referred to National Institute of Standards and Technology (NIST) XPS Databases and related literature.

3. Results and Discussion

3.1. Microflotation

The effect of the concentration of single depressant SHMP and H₃Cit on the recovery of the minerals at a certain collector NaOL concentration (4×10^{-5} mol/L) is depicted in Figure 5. When the concentration of SHMP reached 2×10^{-3} mol/L, although SHMP greatly depressed the flotation of calcite, it also greatly depressed the floatability of scheelite, and the recovery was greatly reduced from 85.7% to 33.6%. This was not conducive to the flotation separation. As shown in Figure 5b, when single H₃Cit was used as the depressant of the scheelite and calcite, the flotation recovery decreased to 40.3% and 54.1% when the H₃Cit concentration reached 2×10^{-3} mol/L. The depression effect of H₃Cit on scheelite was even greater than calcite, which was also not conducive to the flotation separation between scheelite and calcite. Therefore, we considered the combination of two depressants to reveal the depression of the mixed depressant on the minerals.

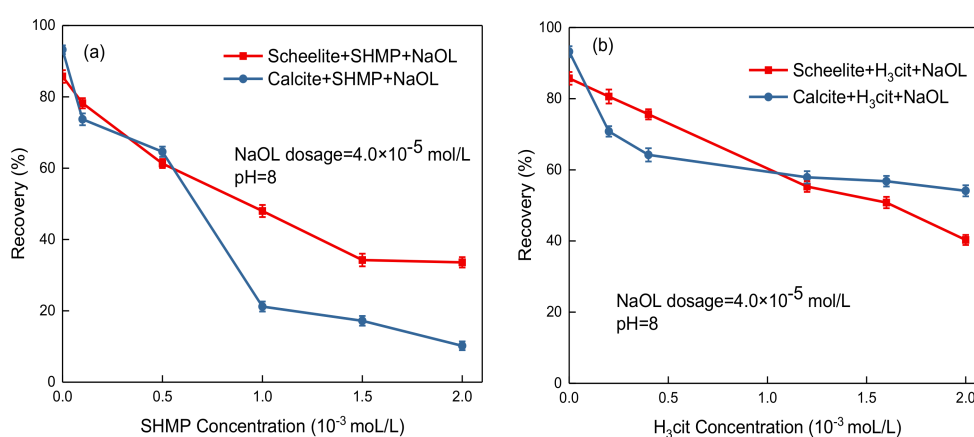


Figure 5. Floatability of minerals as a function of SHMP (a) and H₃Cit (b) concentration.

The effect of the total dosage of mixed depressant of SHMP/H₃Cit on the floatability of minerals is depicted in Figure 6. When the total dosage of the mixed depressant SHMP/H₃Cit was 2×10^{-3} mol/L, the floatability of calcite was greatly reduced to 19.95%, but the scheelite still had a good floatability (61.05%). The large floatability difference between scheelite and calcite under mixed depressant conditions favored the flotation separation between the two minerals. Therefore, from the perspective of flotation selectivity, mixed depressant SHMP/H₃Cit were more advantageous than single depressant SHMP or H₃Cit.

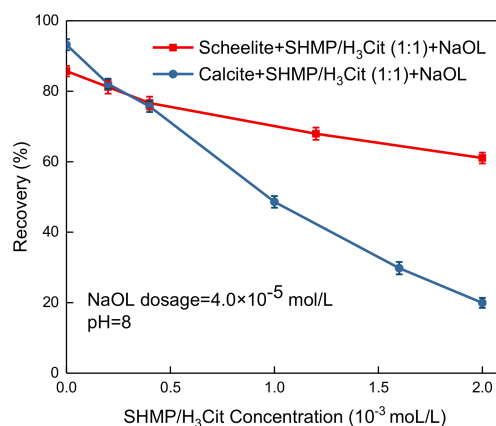


Figure 6. Floatability of minerals as a function of mixed depressant dosage.

The effect of the molar ratio of SHMP to H₃Cit of the mixed depressant on mineral floatability is depicted in Figure 7. The total concentration of mixed depressant was 2×10^{-3} mol/L. As shown in Figure 7, When the molar ratio of SHMP to H₃Cit was 1:4, the floatability of scheelite and calcite were 58.2% and 2.8%, respectively. At this ratio, the difference in floatability between scheelite and calcite was the largest, which was most beneficial to the flotation separation of the two minerals. Therefore, the ratio of 1:4 was the optimum ratio.

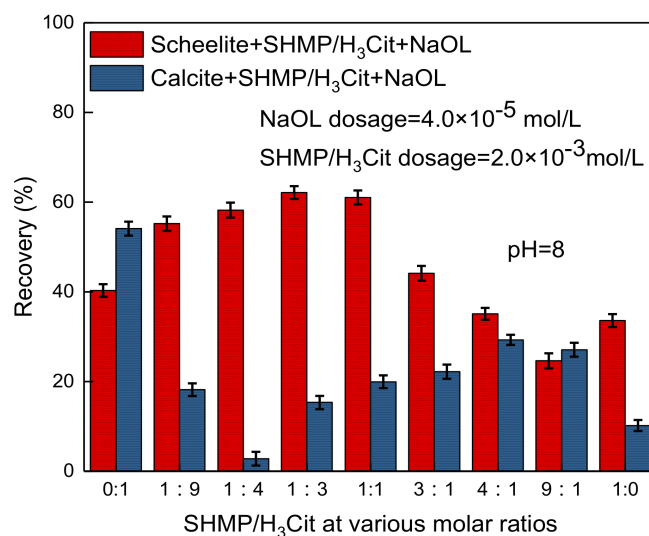


Figure 7. Floatability of minerals with mixed depressants at various molar ratios.

Microflotation results have shown that mixed depressant can achieve good separation effect. To further verify the separation effect of the mixed depressant, the artificial mixed minerals experiments were conducted and the results are shown in Table 1. 2 g of mixed minerals used for this experiment was consisted of 1 g scheelite and 1 g calcite. The dosages of single and mixed depressant were all 1×10^{-3} mol/L. The ratio of SHMP to H₃Cit was 1:4. In the presence of single depressant H₃Cit, a concentrate with scheelite grade of 52.33% was achieved at a recovery of 68.40%. When mixed depressant SHMP/ H₃Cit was used, although the yield of concentrates decreased (from 65.35% to 62.15%), the grade and recovery of scheelite in concentrates increased to 62.19% and 77.3%, respectively. This indicated that the mixed depressant had better selectivity, which was consistent with the microflotation results.

Table 1. Flotation results of artificial mixed minerals.

Depressant	Products	Ratio (%)	Scheelite Grade (%)	Scheelite Recoveries (%)
H ₃ Cit	Concentrates	65.35	52.33	68.40
	Tailing	34.65	45.60	31.60
	Feed	100.00	50.00	100.00
SHMP/H ₃ Cit	Concentrates	62.15	62.19	77.3
	Tailing	37.85	29.98	22.7
	Feed	100.00	50.00	100.00

3.2. Solution Chemistry Analysis

3.2.1. Solution Chemical Calculation of Dissolved Components of Minerals

The dominant components in the mineral slurry are different under different pH conditions. The components in the slurry solution follow the reaction equilibrium, and all reactions follow the proton transfer equilibrium, mass balance and charge balance. Based on these equilibrium reaction relationships, the dominant components in the slurry at different pH conditions can be

calculated. The following reactions exist in the saturated scheelite slurry, and the corresponding reaction equilibrium constants are also listed in Table 2.

Table 2. Reactions and reaction constants in saturated scheelite slurry.

Reactions	Reaction Constants
$H^+ + WO_4^{2-} \rightleftharpoons HWO_4^-$	$K_1^H = 10^{3.5}$ (1)
$H^+ + HWO_4^- \rightleftharpoons H_2WO_4(aq)$	$K_2^H = 10^{4.6}$ (2)
$WO_3(s) + H_2O \rightleftharpoons 2H^+ + WO_4^{2-}$	$K_{s0} = 10^{-14.5}$ (3)
$CaWO_4(s) \rightleftharpoons Ca^{2+} + WO_4^{2-}$	$K_{sp1} = 10^{-9.3}$ (4)
$Ca^{2+} + OH^- \rightleftharpoons CaOH^+$	$K_1 = 10^{1.4}$ (5)
$Ca^{2+} + 2OH^- \rightleftharpoons Ca(OH)_2(aq)$	$K_2 = 10^{2.77}$ (6)
$Ca(OH)_2(s) \rightleftharpoons Ca^{2+} + 2OH^-$	$K_{s1} = 10^{-5.22}$ (7)

For scheelite ($CaWO_4$), the pH at which $Ca(OH)_2$ precipitation begins to be formed is obtained by the following formula:

$$CaWO_4(s) + 2OH^- \rightleftharpoons Ca(OH)_2(s) + WO_4^{2-}$$

$$K'_{11} = \frac{K_{sp1}}{K_{s1}} = 10^{-4.08}$$

$$K'_{11} = \frac{[WO_4^{2-}]}{[OH^-]^2} \implies \frac{\sqrt{K_{sp1}}}{[OH^-]^2} = 10^{-4.08} \implies pH_s = 13.72$$
(8)

The pH at which H_2WO_4 precipitation begins to be formed is obtained by the following formula:

$$CaWO_4(s) + 2H^+ \rightleftharpoons H_2WO_4(s) + Ca^{2+}$$

$$K'_{12} = \frac{K_{sp1}}{K_{s0}} = 10^{-4.75}$$

$$K'_{12} = \frac{[Ca^{2+}]}{[H^+]^2} \implies \frac{\sqrt{K_{sp1}}}{[H^+]^2} = 10^{-4.75} \implies pH_m = 4.7$$
(9)

After calculation, the relationship between the concentration (C) of each component of saturated scheelite and pH is shown in Table 3.

Table 3. Relationship between the concentration (C) and pH.

log C	pH < 4.7	pH = 4.7–13.72	pH < 13.72
$[Ca^{2+}]$	4.75-2 pH	$\frac{1}{2}[\log K_{sp1} + \log \alpha_{WO_4^{2-}} - \log \alpha_{Ca^{2+}}]$	22.78-2 pH
$[CaOH^+]$	-7.85-pH	$-12.6+pH + \log[Ca^{2+}]$	10.18-pH
$[Ca(OH)_2(aq.)]$	-20.48	$-25.23+2pH + \log[Ca^{2+}]$	-2.45
$[WO_4^{2-}]$	-14.05 + 2 pH	$\frac{1}{2}[\log K_{sp1} + \log \alpha_{Ca^{2+}} - \log \alpha_{WO_4^{2-}}]$	13.48 + 2pH
$[HWO_4^-]$	-10.55 + pH	$3.5-pH + \log[WO_4^{2-}]$	16.98 + pH
$[H_2WO_4(aq.)]$	-5.95	$8.1-2pH + \log[WO_4^{2-}]$	

In Table 3, $\alpha_{WO_4^{2-}}$ and $\alpha_{Ca^{2+}}$ are the side reaction coefficients of WO_4^{2-} and Ca^{2+} , and the calculation formulas are:

$$\alpha_{WO_4^{2-}} = 1 + K_1^H [H^+] + K_1^H K_2^H [H^+]^2$$
(10)

$$\alpha_{Ca^{2+}} = 1 + K_1 [OH^-] + K_2 [OH^-]^2$$
(11)

From the formulas in Table 3 and Formulas (10) and (11), the logarithmic of the concentration of each component in the saturated solution of scheelite can be calculated, and the figure is shown in Figure 8a.

In addition to Formulas (5) to (7), the equilibrium reactions and equilibrium constants in the saturated solution of calcite are shown in Table 4.

Table 4. Reactions and corresponding reaction constants in saturated calcite slurry.

Reactions	Reaction Constants
$\text{CaCO}_3 (\text{s}) \rightleftharpoons \text{Ca}^{2+} + \text{CO}_3^{2-}$	$K_{\text{sp}2} = 10^{-3.35}$ (12)
$\text{H}^+ + \text{CO}_3^{2-} \rightleftharpoons \text{HCO}_3^-$	$K_3^{\text{H}} = 10^{10.33}$ (13)
$\text{H}^+ + \text{HCO}_3^- \rightleftharpoons \text{H}_2\text{CO}_3 (\text{aq.})$	$K_4^{\text{H}} = 10^{6.35}$ (14)
$\text{H}_2\text{CO}_3 \rightleftharpoons \text{CO}_2 (\text{g}) + \text{H}_2\text{O}$	$K_3 = 10^{1.47}$ (15)
$\text{Ca}^{2+} + \text{CO}_3^{2-} \rightleftharpoons \text{CaCO}_3 (\text{aq.})$	$K_4 = 10^{3.35}$ (16)
$\text{Ca}^{2+} + \text{HCO}_3^- \rightleftharpoons \text{CaHCO}_3^+$	$K_5 = 10^{0.82}$ (17)

In the atmosphere, take $P_{\text{CO}_2} = 10^{-3.5}$ atm (standard atmospheric pressure), so $[\text{H}_2\text{CO}_3 (\text{aq.})] = \frac{P_{\text{CO}_2}}{K_3} = 10^{-4.97}$. According to the reaction Formulas (5) to (7) and the reaction Formulas (12) to (17), the logarithmic of the concentration of other components in the saturated solution of calcite can be calculated as follows:

$$\log [\text{HCO}_3^-] = -11.31 + \text{pH}$$

$$\log [\text{CO}_3^{2-}] = -21.65 + 2\text{pH}$$

$$\log [\text{CaCO}_3 (\text{aq.})] = -5.09$$

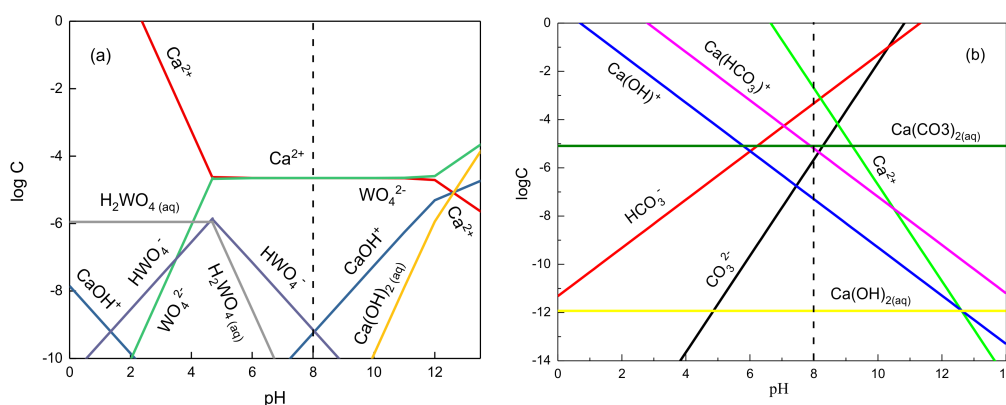
$$\log [\text{Ca}^{2+}] = 13.3 - 2\text{pH}$$

$$\log [\text{CaOH}^+] = 0.7 - \text{pH}$$

$$\log [\text{Ca}(\text{OH})_2 (\text{aq.})] = -11.93$$

$$\log [\text{CaHCO}_3^+] = 2.8 - \text{pH}$$

Therefore, the logC-pH diagram of calcite can be obtained (Figure 8b).

**Figure 8.** Species distribution diagrams of scheelite (a) and calcite (b).

As depicted in Figure 8a, When the pH was 8, the positioning ions on the surface of the saturated scheelite solution were WO_4^{2-} and Ca^{2+} . This was consistent with previous related literature [14]. As shown in Figure 8b, the positioning ion on the surface of the saturated calcite solution was mainly Ca^{2+} at pH 8, which made the surface of the calcite positively charged. This also agreed with related literature [6].

3.2.2. Solution Chemical Calculation of Components of SHMP and H_3Cit Solution

The concentration of each component as a percentage of the total concentration in the SHMP and H_3Cit solution is the distribution coefficient of each component. The dominant components of the dissolved reagents in the slurry determine the adsorption between the reagents and the minerals.

The equilibrium reaction formulas and corresponding reaction coefficients in SHMP and H₃Cit solution are shown in Table 5.

Table 5. Reactions and corresponding reaction constants.

Reactions	Reaction Constants
$H^+ + PO_4^{3-} \rightleftharpoons HPO_4^{2-}$	$K_{11}^H = 10^{12.35}$ (18)
$H^+ + HPO_4^{2-} \rightleftharpoons H_2PO_4^-$	$K_{12}^H = 10^{7.2}$ (19)
$H^+ + H_2PO_4^- \rightleftharpoons H_3PO_4$	$K_{13}^H = 10^{2.15}$ (20)
$H^+ + Cit^{3-} \rightleftharpoons HCit^{2-}$	$K_{21}^H = 10^{6.396}$ (21)
$H^+ + HCit^{2-} \rightleftharpoons H_2Cit^-$	$K_{22}^H = 10^{4.761}$ (22)
$H^+ + H_2Cit^- \rightleftharpoons H_3Cit$	$K_{23}^H = 10^{3.31}$ (23)

The side reaction coefficients of PO_4^{3-} and Cit^{3-} are $\alpha_{PO_4^{3-}}$ and $\alpha_{Cit^{3-}}$, and the calculation formulas are:

$$\alpha_{PO_4^{3-}} = 1 + K_{11}^H [H^+] + K_{11}^H K_{12}^H [H^+]^2 + K_{11}^H K_{12}^H K_{13}^H [H^+]^3 \quad (24)$$

$$\alpha_{Cit^{3-}} = 1 + K_{21}^H [H^+] + K_{21}^H K_{22}^H [H^+]^2 + K_{21}^H K_{22}^H K_{23}^H [H^+]^3 \quad (25)$$

The distribution coefficients of every component in SHMP and H₃Cit solution are calculated as follows [41]:

$$\Phi_{PO_4^{3-}} = 1/\alpha_{PO_4^{3-}} = 1/(1 + K_{11}^H [H^+] + K_{11}^H K_{12}^H [H^+]^2 + K_{11}^H K_{12}^H K_{13}^H [H^+]^3) \quad (26)$$

$$\Phi_{HPO_4^{2-}} = K_{11}^H [H^+] \Phi_{PO_4^{3-}} \quad (27)$$

$$\Phi_{H_2PO_4^-} = K_{11}^H K_{12}^H [H^+]^2 \Phi_{PO_4^{3-}} \quad (28)$$

$$\Phi_{H_3PO_4} = K_{11}^H K_{12}^H K_{13}^H [H^+]^3 \Phi_{PO_4^{3-}} \quad (29)$$

$$\Phi_{Cit^{3-}} = 1/\alpha_{Cit^{3-}} = 1/(1 + K_{21}^H [H^+] + K_{21}^H K_{22}^H [H^+]^2 + K_{21}^H K_{22}^H K_{23}^H [H^+]^3) \quad (30)$$

$$\Phi_{HCit^{2-}} = K_{21}^H [H^+] \Phi_{Cit^{3-}} \quad (31)$$

$$\Phi_{H_2Cit^-} = K_{21}^H K_{22}^H [H^+]^2 \Phi_{Cit^{3-}} \quad (32)$$

$$\Phi_{H_3Cit} = K_{21}^H K_{22}^H K_{23}^H [H^+]^3 \Phi_{Cit^{3-}} \quad (33)$$

The distribution coefficient diagram of every component of SHMP and H₃Cit solution can be calculated from the above series of formulas, as shown in Figure 9.

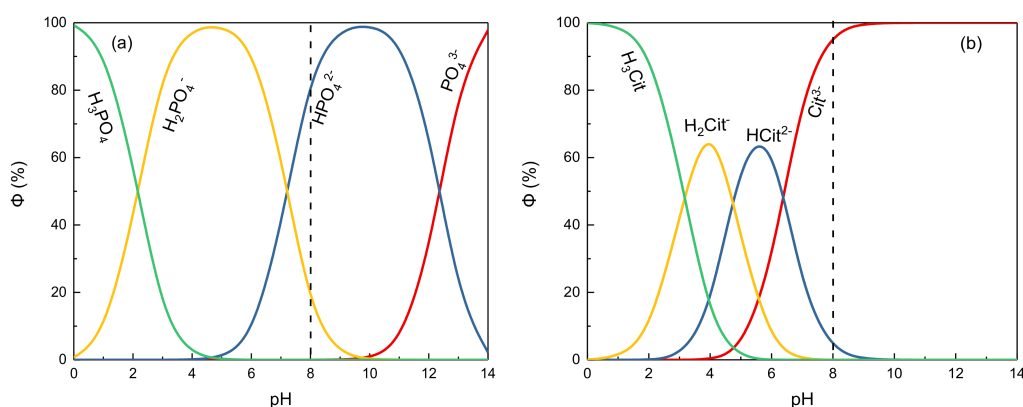


Figure 9. Distribution coefficients of components in SHMP (a) and H₃Cit (b) solution.

As depicted in Figure 9a, the dominant component in the SHMP solution was HPO_4^{2-} at pH 8. Under this condition, Chelation of HPO_4^{2-} and Ca^{2+} formed CaHPO_4 when SHMP was adsorbed on the mineral surfaces. As shown in Figure 9b, the main species in H_3Cit solution at pH 8 was Cit^{3-} . When H_3Cit was interacted with the minerals, the dominant component Cit^{3-} and Ca^{2+} bonded to form $\text{Ca}_3(\text{Cit})_2$ on the mineral surfaces. The adsorption strength of SHMP and H_3Cit was revealed with a further zeta potential experiment and thermodynamic analyses.

3.3. Zeta Potential Analysis

The zeta potential of minerals under different depressants is shown in Figure 10, respectively. The concentration of the single depressant (SHMP or H_3Cit) and the mixed depressant SHMP/ H_3Cit were both 2×10^{-3} mol/L. As shown in Figure 10a, bare scheelite had a negative zeta potential in ultrapure water over the entire pH range (6.5–10.2), which was consistent with previous study [6]. According to the solution chemistry calculation of scheelite, the positioning ions on the surface of scheelite were mainly WO_4^{2-} and Ca^{2+} at pH 8. Considering that the surface zeta potential was negative under this condition, the dominant component of the scheelite surface was mainly WO_4^{2-} . Under the conditioning of depressant SHMP or H_3Cit , the zeta potential of scheelite was decreased, indicating that the negatively charged HPO_4^{2-} and Cit^{3-} in the SHMP and H_3Cit solutions specific adsorbed on the scheelite surface with the negative charge. After the conditioning of the mixed depressant SHMP/ H_3Cit , the magnitude of the decrease in the zeta potential of the scheelite was small, indicating that the adsorption of the mixed depressant on the surface of the scheelite was weak.

The zeta potential of calcite under different reagent conditions is shown in Figure 10b. The isoelectric point (IEP) of pure calcite appeared at around 9.3, which was consistent with the relevant literature [44,45]. Combined with the solution chemical calculation results of the calcite, the dominant component of the calcite surface was Ca^{2+} . Depressant SHMP or H_3Cit was adsorbed on the calcite surface, and the zeta potential was negatively shifted, indicating that the negatively charged components HPO_4^{2-} and Cit^{3-} were chemically adsorbed on the surface of calcite. The mixed depressant SHMP/ H_3Cit reduced the zeta potential of calcite to a greater extent, indicating that the mixed depressant had co-adsorbed on the calcite surface, and the adsorption on the calcite surface was more intense than scheelite.

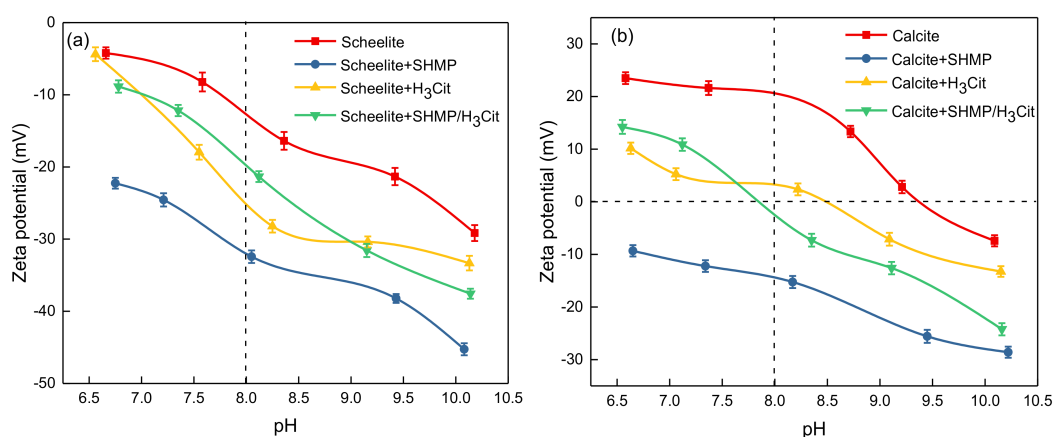


Figure 10. Zeta potential of minerals with different reagents. (a) scheelite, (b) calcite.

3.4. Thermodynamic Analyses

In order to better explain the flotation phenomenon, the Gibbs free energy change of the reaction between the depressants (SHMP and H_3Cit) and the minerals (scheelite and calcite) was calculated. From the above solution chemistry results, SHMP and H_3Cit reacted with calcium ions on the mineral surface to form CaHPO_4 and $\text{Ca}_3(\text{Cit})_2$ precipitates at pH 8, respectively.

In the scheelite and calcite solution, the equilibrium reactions and equilibrium constants between the corresponding components of SHMP and calcium ions are depicted in Table 6. The Formulas (4) to (6) and Formulas (18) to (20) are shown in Tables 2 and 5, respectively, and are not listed in Table 6.

Table 6. Reactions and corresponding reaction constants.

Reactions	Reaction Constants
$\text{Ca}^{2+} + \text{HPO}_4^{2-} \rightleftharpoons \text{CaHPO}_4 (\text{s})$	$K_{\text{sp}3} = 10^{-6.58}$ (34)
$\text{Ca}^{2+} + \text{PO}_4^{3-} \rightleftharpoons \text{CaPO}_4^-$	$K_6 = 10^{6.46}$ (35)
$\text{Ca}^{2+} + \text{HPO}_4^{2-} \rightleftharpoons \text{CaHPO}_4 (\text{aq.})$	$K_7 = 10^{2.74}$ (36)
$\text{Ca}^{2+} + \text{H}_2\text{PO}_4^- \rightleftharpoons \text{CaH}_2\text{PO}_4^+$	$K_8 = 10^{1.4}$ (37)

The formula of Gibbs free energy change can be obtained from the equilibrium reaction (34), as follows:

$$\Delta G = RT \ln K_{\text{sp}3} \alpha'_{\text{Ca}^{2+}} \alpha_{\text{HPO}_4^{2-}} - RT \ln [\text{Ca}^{2+}] [\text{HPO}_4^{2-}] \quad (38)$$

where R represents the ideal gas constant ($8.314 \text{ J} \times \text{mol}^{-1} \times \text{K}^{-1}$); T represents standard thermodynamic temperature (298.15K); $\alpha_{\text{HPO}_4^{2-}}$ and $\alpha'_{\text{Ca}^{2+}}$ represent the side reaction coefficients of HPO_4^{2-} and Ca^{2+} in this system, respectively; $[\text{HPO}_4^{2-}]$ and $[\text{Ca}^{2+}]$ are the concentration of HPO_4^{2-} and Ca^{2+} ; C_T is the concentration of SHMP ($2 \times 10^{-3} \text{ mol/L}$). The relevant parameters are calculated as follows:

$$\alpha_{\text{PO}_4^{3-}} = 1 + K_{11}^{\text{H}} [\text{H}^+] + K_{11}^{\text{H}} K_{12}^{\text{H}} [\text{H}^+]^2 + K_{11}^{\text{H}} K_{12}^{\text{H}} K_{13}^{\text{H}} [\text{H}^+]^3 \quad (24)$$

$$\alpha_{\text{HPO}_4^{2-}} = \frac{\alpha_{\text{PO}_4^{3-}} - 1}{K_{11}^{\text{H}} [\text{H}^+]} \quad (39)$$

$$\alpha'_{\text{Ca}^{2+}} = 1 + K_6 [\text{PO}_4^{3-}] + K_7 K_{11}^{\text{H}} [\text{PO}_4^{3-}] [\text{H}^+] + K_8 K_{11}^{\text{H}} K_{12}^{\text{H}} [\text{PO}_4^{3-}] [\text{H}^+]^2 + K_1 [\text{OH}^-] + K_2 [\text{OH}^-]^2 \quad (40)$$

$$[\text{HPO}_4^{2-}] = \frac{C_T}{\alpha_{\text{PO}_4^{3-}}} K_{11}^{\text{H}} [\text{H}^+] \quad (41)$$

For the reactions between scheelite and SHMP, the calcium ion concentration is calculated as follows:

$$[\text{Ca}^{2+}] = \sqrt{\frac{K_{\text{sp}1} \alpha_{\text{WO}_4^{2-}}}{\alpha_{\text{Ca}^{2+}}}} \quad (42)$$

For the reactions between calcite and SHMP, the calcium ion concentration is calculated as follows:

$$[\text{Ca}^{2+}] = 10^{13.31-2\text{pH}} \quad (43)$$

As such, according to the reaction Formulas (4) to (6), (18) to (20), (24), and the reaction formulas (34) to (43), the Gibbs free energy change of the reactions between scheelite and calcite with SHMP can be calculated, as shown in Figure 11.

In the scheelite and calcite solution, the equilibrium reactions and equilibrium constants between the corresponding components of H_3Cit and calcium ions are depicted in Table 7. The formulas (4) to (6) and formulas (21) to (23) are shown in Tables 2 and 5, respectively, and are not listed in Table 7.

Table 7. Reactions and corresponding reaction constants.

Reactions	Reaction Constants
$\text{Ca}_3\text{Cit}_2(\text{s}) \rightleftharpoons 3\text{Ca}^{2+} + 2\text{Cit}^{3-}$	$K_{\text{sp}4} = 5 \times 10^{-7}$ (44)
$\text{Ca}^{2+} + \text{Cit}^{3-} \rightleftharpoons \text{CaCit}^-$	$K_9 = 10^{4.68}$ (45)
$\text{Ca}^{2+} + \text{HCit}^{2-} \rightleftharpoons \text{CaHCit}(\text{aq})$	$K_{10} = 10^{3.09}$ (46)
$\text{Ca}^{2+} + \text{H}_2\text{Cit}^- \rightleftharpoons \text{CaH}_2\text{Cit}^+$	$K_{11} = 10^{1.1}$ (47)

The formula of Gibbs free energy change can be obtained from the equilibrium reaction (44). The meaning of the relevant parameters refers to the above section.

$$\Delta G = RT \ln K_{\text{sp}4} \alpha_{\text{Ca}^{2+}}^3 \alpha_{\text{Cit}^{3-}}^2 - RT \ln [\text{Ca}^{2+}]^3 [\text{Cit}^{3-}]^2 \quad (48)$$

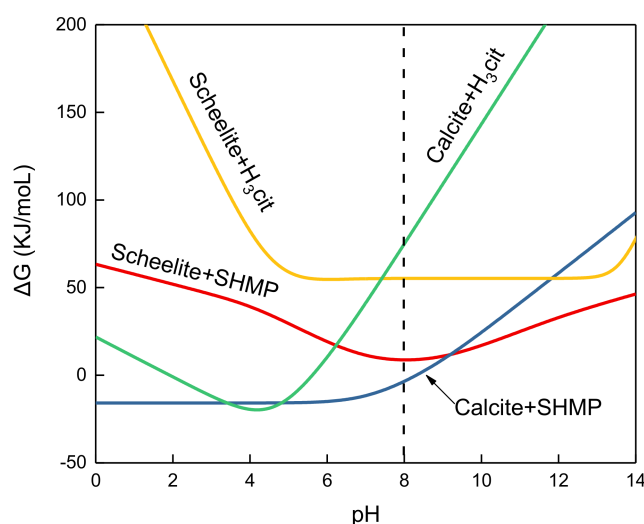
$$\alpha_{\text{Ca}^{2+}}' = 1 + K_9 [\text{Cit}^{3-}] + K_{10} K_{21}^{\text{H}} [\text{Cit}^{3-}] [\text{H}^+] + K_{11} K_{21}^{\text{H}} K_{22}^{\text{H}} [\text{Cit}^{3-}] [\text{H}^+]^2 + K_1 [\text{OH}^-] + K_2 [\text{OH}^-]^2 \quad (49)$$

$$\alpha_{\text{Cit}^{3-}} = 1 + K_{21}^{\text{H}} [\text{H}^+] + K_{21}^{\text{H}} K_{22}^{\text{H}} [\text{H}^+]^2 + K_{21}^{\text{H}} K_{22}^{\text{H}} K_{23}^{\text{H}} [\text{H}^+]^3 \quad (25)$$

$$[\text{Cit}^{3-}] = \frac{C_{\text{T}}}{\alpha_{\text{Cit}^{3-}}} \quad (50)$$

For the reactions between minerals (scheelite and calcite) and H_3Cit , the calcium ion concentration is still calculated according to formulas (42) and (43).

According to the reaction Formulas (4) to (6), (21) to (23), (25), and the reaction Formulas (42) to (50), the ΔG of the reactions between scheelite and calcite with H_3Cit can be calculated, as shown in Figure 11. The ΔG of the reaction when CaHPO_4 precipitate was formed on calcite surface was smaller than that on scheelite surface at pH 8. Therefore, the precipitation of CaHPO_4 was easier to be formed on the calcite surface, so the depressant effect of SHMP on the calcite was stronger than that of the scheelite. The ΔG of the reaction when $\text{Ca}_3(\text{Cit})_2$ precipitate was formed was bigger than that when CaHPO_4 precipitate was formed, illustrating that SHMP had a stronger depressive effect on minerals than H_3Cit .

**Figure 11.** The ΔG as a function of pH for the reaction of depressants with minerals.

3.5. XPS Analysis

The relative concentrations and the shifts of mineral surface elements (before and after the conditioning of corresponding depressants) tested by XPS are shown in Table 8. The relative concentration was the relative concentration percentage between the elements being characterized.

After the conditioning of depressant H₃Cit with the minerals, the relative content of the C and O elements on the mineral surfaces became larger due to the adsorption of H₃Cit, but the relative content of the Ca element became smaller. The decrease in the relative content of Ca was mainly due to the increase in the relative content of the corresponding C and O elements. When SHMP was used as a depressant, the relative contents of P element on the scheelite and calcite surfaces increased by 2.76% and 3.00%. This indicated that SHMP had similar depressive effect on scheelite and calcite. When scheelite interacted by the mixed depressant SHMP/H₃Cit, the relative content of the P element increased by 2.16%, less than 2.76%, indicating that the adsorption amount of SHMP in the mixed depressant on scheelite surface was smaller than that of the single depressant SHMP. Because the relative contents of the C and O elements were reduced (−0.72% and −0.53%), the adsorption of H₃Cit in the mixed depressant SHMP/H₃Cit on the surface of the scheelite was also very weak. In contrast, the relative content of P element on the surface of calcite treated by the mixed depressant was increased by 4.12%, much larger than the surface of scheelite (2.16%) and the surface of the calcite after the reaction of single SHMP (3.00%). This indicated that the SHMP in the mixed depressant was more strongly adsorbed on the calcite surface than that of scheelite. In addition, the adsorption strength of SHMP in the mixed depressant on the surface of calcite was also larger than that of the single depressant SHMP. In contrast to scheelite, the relative contents of C and O elements on the surface of the calcite increased after adding of SHMP/H₃Cit, indicating that the H₃Cit in the mixed depressant was also adsorbed on calcite surface. This demonstrated the co-adsorption of SHMP and H₃Cit occurred on the calcite surface. It was indicated that the mixed depressant had a strong depressive effect on the calcite.

Table 8. Atomic relative content and the corresponding shifts.

Samples.	Relative Content (%)			
	Ca 2p	C 1s	O 1s	P 2p
Scheelite	13.61	32.77	53.62	-
Scheelite + H ₃ Cit	12.86	33.09	54.05	-
Scheelite + SHMP	12.23	31.65	53.36	2.76
Scheelite + SHMP/H ₃ Cit	12.70	32.05	53.09	2.16
D _S -H ₃ Cit	−0.75	+0.32	+0.43	-
D _S -SHMP	−1.38	−1.12	−0.26	+2.76
D _S -SHMP/H ₃ Cit	−0.91	−0.72	−0.53	+2.16
Calcite	15.43	37.97	46.60	-
Calcite + H ₃ Cit	14.94	38.06	47.00	-
Calcite + SHMP	14.01	36.67	46.32	3.00
Calcite + H ₃ Cit/SHMP	10.66	38.15	47.07	4.12
D _c -H ₃ Cit	−0.49	+0.09	+0.40	-
D _c -SHMP	−1.42	−1.30	−0.28	+3.00
D _c -SHMP/H ₃ Cit	−4.77	+0.18	+0.47	+4.12

The separated and fitting of the peaks of O 1s on calcite surface after the conditioning of the mixed depressant are shown in Figure 12. According to the NIST XPS Databases and related literatures [42,46,47], the peak at 531.22 eV was contributed by the oxygen in the CO₃^{2−} of the calcite. The peak at 532.55 eV was probably the binding energy of the oxygen in the Ca-COOR, indicating that the depressant H₃Cit of the mixed depressant was absorbed on the calcite surface. Moreover, the peak at 533.42 eV was assigned to PO₄^{3−} of the SHMP, indicating that the depressant SHMP of the mixed depressant was also absorbed on the calcite surface. This indicated that the SHMP and H₃Cit in the mixed depressant were co-adsorbed on calcite surface. Therefore, the depressive effect of mixed depressant on calcite was strong.

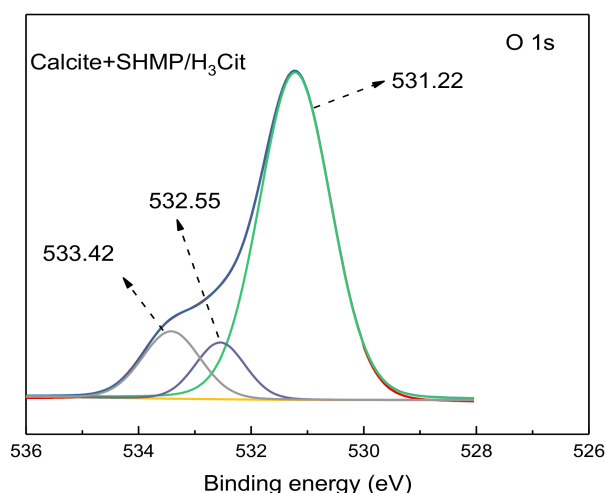


Figure 12. Fitting peaks of Ca 2p 3/2 on mineral surfaces.

3.6. Adsorption Model

According to the experimental mechanism that has been studied, a possible adsorption model of the mixed depressant SHMP/H₃Cit and collector NaOL on the mineral surfaces can be obtained. The advantage of the mixed depressant is mainly reflected in the stronger flotation selectivity on the two minerals. This is reflected in the difference in the adsorption behavior of the mixed depressant on the scheelite and calcite surfaces. As depicted in Figure 13, after the mixed depressant interacted with the minerals, SHMP and H₃Cit in the mixed depressant are co-adsorbed on calcite surface, and this hindered further adsorption of the collector NaOL. This made the floatability of calcite very strongly depressed. However, the adsorption of mixed depressant on scheelite surface was very weak, particularly, the H₃Cit of the mixed depressant had weak adsorption on the surface of scheelite. This made the floatability of scheelite less affected.

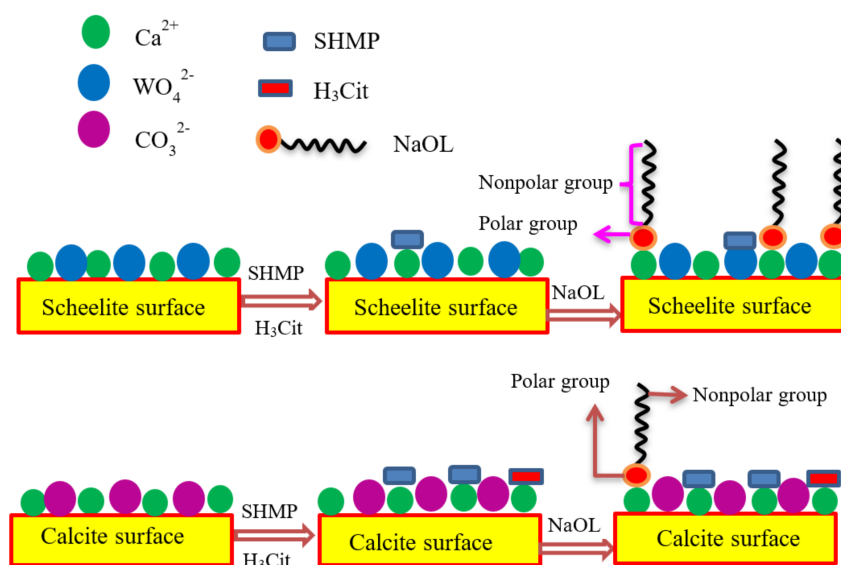


Figure 13. Schematic diagram of adsorption model of reagents on scheelite and calcite.

4. Conclusions

The single depressant SHMP or H₃Cit cannot achieve the flotation separation between scheelite and calcite because of their poor selectivity. When the mixed depressant SHMP/ H₃Cit was used, the flotation recovery of scheelite and calcite reached 58.2% and 2.8% at an optimum molar ratio of

1:4, respectively, and the flotation separation could be achieved. Artificial mixed mineral experiment indicated that the mixed depressant can significantly improve the separation efficiency of scheelite and calcite. The depressants SHMP and H₃Cit were chemically bonded with the calcium ions on the mineral surface to form CaHPO₄ and Ca₃(Cit)₂, respectively. Thermodynamic analysis indicated that the CaHPO₄ was easier to form than Ca₃(Cit)₂ on the mineral surfaces, indicating that the depressive effect of SHMP was stronger than H₃Cit. XPS indicated that SHMP and H₃Cit of the mixed depressant were co-adsorbed on calcite surface, while H₃Cit of mixed depressant was weakly adsorbed on scheelite surface. The mixed depressant SHMP/ H₃Cit had a stronger depressive effect on calcite than scheelite, and the flotation separation efficiency of scheelite from calcite can be improved.

Author Contributions: Data curation, W.Z. and L.D.; Funding acquisition, F.J. and W.Q.; Investigation, Q.W.; Methodology, L.D., F.J. and Q.W.; Project administration, W.Q.; Resources, W.Z. and W.Q.; Software, Q.W.; Supervision, F.J. and W.Q.; Writing—original draft, W.Z.; Writing—review & editing, L.D.

Funding: The authors gratefully acknowledge the financial support of this research by Provincial Science and technology leader (Innovation team of interface chemistry of efficient and clean utilization of complex mineral resources, Grant No. 2016RS2016); National Natural Science Foundation of China (Project No. 51604302 and No. 51574282); and the Key laboratory of Hunan Province for Clean and Efficiency Utilization of strategic Calcium-containing mineral Resources (No. 2018TP1002).

Conflicts of Interest: The authors declare no conflict of interest.

References

1. Yang, X.; Ai, G. Effects of surface electrical property and solution chemistry on fine wolframite flotation. *Sep. Purif. Technol.* **2016**, *170*, 272–279. [[CrossRef](#)]
2. Singh, H.; Pandey, O.P. Novel process for synthesis of nanocrystalline WC from wolframite ore. *Ceram. Int.* **2015**, *41*, 10481–10487. [[CrossRef](#)]
3. Harlaux, M.; Mercadier, J.; Marignac, C.; Peiffert, C.; Cloquet, C.; Cuney, M. Tracing metal sources in peribatholithic hydrothermal W deposits based on the chemical composition of wolframite: The example of the Variscan French Massif Central. *Chem. Geol.* **2018**, *479*, 58–85. [[CrossRef](#)]
4. Oliveira, M.C.; Andrés, J.; Gracia, L.; de Oliveira, M.S.M.P.; Mercury, J.M.R.; Longo, E.; Nogueira, I.C. Geometry, electronic structure, morphology, and photoluminescence emissions of BaW_{1-x}MoxO₄ (x = 0, 0.25, 0.50, 0.75, and 1) solid solutions: Theory and experiment in concert. *Appl. Surf. Sci.* **2019**, *463*, 907–917. [[CrossRef](#)]
5. Li, C.; Gao, Z. Tune surface physicochemical property of fluorite particles by regulating the exposure degree of crystal surfaces. *Miner. Eng.* **2018**, *128*, 123–132. [[CrossRef](#)]
6. Dong, L.; Jiao, F.; Qin, W.; Zhu, H.; Jia, W. New insights into the carboxymethyl cellulose adsorption on scheelite and calcite: Adsorption mechanism, AFM imaging and adsorption model. *Appl. Surf. Sci.* **2019**, *463*, 105–114. [[CrossRef](#)]
7. Xu, L.; Tian, J.; Wu, H.; Fang, S.; Lu, Z.; Ma, C.; Sun, W.; Hu, Y. Anisotropic surface chemistry properties and adsorption behavior of silicate mineral crystals. *Adv. Colloid Interface Sci.* **2018**, *256*, 340–351. [[CrossRef](#)]
8. Xu, L.; Tian, J.; Wu, H.; Lu, Z.; Sun, W.; Hu, Y. The flotation and adsorption of mixed collectors on oxide and silicate minerals. *Adv. Colloid Interface Sci.* **2017**, *250*, 1–14. [[CrossRef](#)]
9. Xu, L.; Hu, Y.; Tian, J.; Wu, H.; Yang, Y.; Zeng, X.; Wang, Z.; Wang, J. Selective flotation separation of spodumene from feldspar using new mixed anionic/cationic collectors. *Miner. Eng.* **2016**, *89*, 84–92. [[CrossRef](#)]
10. Rhamdhani, M.A.; Ahmad, S.; Pownceby, M.I.; Bruckard, W.J.; Harjanto, S. Selective sulphidation of impurities in weathered ilmenite. Part 1—Applicability to different ilmenite deposits and simulated Becher kiln conditions. *Miner. Eng.* **2018**, *121*, 55–65. [[CrossRef](#)]
11. Mehdilo, A.; Irannajad, M.; Rezai, B. Effect of crystal chemistry and surface properties on ilmenite flotation behavior. *Int. J. Miner. Process.* **2015**, *137*, 71–81. [[CrossRef](#)]
12. Parapari, P.S.; Irannajad, M.; Mehdilo, A. Effect of acid surface dissolution pretreatment on the selective flotation of ilmenite from olivine and pyroxene. *Int. J. Miner. Process.* **2017**, *167*, 49–60. [[CrossRef](#)]
13. Gao, Z.; Fan, R.; Ralston, J.; Sun, W.; Hu, Y. Surface broken bonds: An efficient way to assess the surface behaviour of fluorite. *Miner. Eng.* **2019**, *130*, 15–23. [[CrossRef](#)]

14. Chen, W.; Feng, Q.; Zhang, G.; Yang, Q. Investigations on flotation separation of scheelite from calcite by using a novel depressant: Sodium phytate. *Miner. Eng.* **2018**, *126*, 116–122. [[CrossRef](#)]
15. Filippov, L.O.; Foucaud, Y.; Filippova, I.V.; Badawi, M. New reagent formulations for selective flotation of scheelite from a skarn ore with complex calcium minerals gangue. *Miner. Eng.* **2018**, *123*, 85–94. [[CrossRef](#)]
16. Medeiros, A.R.S.D.; Baltar, C.A.M. Importance of collector chain length in flotation of fine particles. *Miner. Eng.* **2018**, *122*, 179–184. [[CrossRef](#)]
17. Abarca, C.; Ali, M.M.; Pelton, R.H. Choosing mineral flotation collectors from large nanoparticle libraries. *J. Colloid Interface Sci.* **2018**, *516*, 423–430. [[CrossRef](#)]
18. Zhang, C.; Sun, W.; Hu, Y.; Tang, H.; Yin, Z.; Guan, Q.; Gao, J. Investigation of two-stage depressing by using hydrophilic polymer to improve the process of fluorite flotation. *J. Clean. Prod.* **2018**, *193*, 228–235. [[CrossRef](#)]
19. Feng, B.; Zhang, W.; Guo, Y.; Peng, J.; Ning, X.; Wang, H. Synergistic effect of acidified water glass and locust bean gum in the flotation of a refractory copper sulfide ore. *J. Clean. Prod.* **2018**, *202*, 1077–1084. [[CrossRef](#)]
20. Liu, J.; Li, E.-L.; Jiang, K.; Li, Y.-J.; Han, Y.-X. Effect of acidic activators on the flotation of oxidized pyrrhotite. *Miner. Eng.* **2018**, *120*, 75–79. [[CrossRef](#)]
21. Liu, C.; Zhang, W.; Song, S.; Li, H. A novel method to improve carboxymethyl cellulose performance in the flotation of talc. *Miner. Eng.* **2019**, *131*, 23–27. [[CrossRef](#)]
22. Liu, C.; Zhu, G.; Song, S.; Li, H. Flotation separation of smithsonite from quartz using calcium lignosulphonate as a depressant and sodium oleate as a collector. *Miner. Eng.* **2019**, *131*, 385–391. [[CrossRef](#)]
23. Bo, F.; Luo, X.; Wang, J.; Wang, P. The flotation separation of scheelite from calcite using acidified sodium silicate as depressant. *Miner. Eng.* **2015**, *80*, 45–49. [[CrossRef](#)]
24. Gao, Y.; Gao, Z.; Sun, W.; Yin, Z.; Wang, J.; Hu, Y. Adsorption of a novel reagent scheme on scheelite and calcite causing an effective flotation separation. *J. Colloid Interface Sci.* **2017**, *512*, 39–46. [[CrossRef](#)] [[PubMed](#)]
25. Zhang, Y.; Chen, R.; Li, Y.; Wang, Y.; Luo, X. Flotation separation of scheelite from calcite using sodium polyacrylate as depressant. *Physicochem. Probl. Miner. Process.* **2018**, *54*, 505–516.
26. Wang, J.; Bai, J.; Yin, W.; Liang, X. Flotation separation of scheelite from calcite using carboxyl methyl cellulose as depressant. *Miner. Eng.* **2018**, *127*, 329–333. [[CrossRef](#)]
27. Power, O.M.; Fenelon, M.A.; O'Mahony, J.A.; McCarthy, N.A. Dephosphorylation of caseins in milk protein concentrate alters their interactions with sodium hexametaphosphate. *Food Chem.* **2019**, *271*, 136–141. [[CrossRef](#)]
28. Asamoah, R.K.; Skinner, W.; Addai-Mensah, J. Leaching behaviour of mechano-chemically activated bio-oxidised refractory flotation gold concentrates. *Powder Technol.* **2018**, *331*, 258–269. [[CrossRef](#)]
29. Han, Y.; Liu, W.; Zhou, J.; Chen, J. Interactions between kaolinite Al OH surface and sodium hexametaphosphate. *Appl. Surf. Sci.* **2016**, *387*, 759–765. [[CrossRef](#)]
30. Neves, J.G.; Danelon, M.; Pessan, J.P.; Figueiredo, L.R.; Camargo, E.R.; Delbem, A.C.B. Surface free energy of enamel treated with sodium hexametaphosphate, calcium and phosphate. *Arch. Oral Biol.* **2018**, *90*, 108–112. [[CrossRef](#)]
31. Liang, L.; Zhang, T.; Peng, Y.; Xie, G. Inhibiting heterocoagulation between microcrystalline graphite and quartz by pH modification and sodium hexametaphosphate. *Colloids Surf. A Physicochem. Eng. Asp.* **2018**, *553*, 149–154. [[CrossRef](#)]
32. Ramirez, A.; Rojas, A.; Gutierrez, L.; Laskowski, J.S. Sodium hexametaphosphate and sodium silicate as dispersants to reduce the negative effect of kaolinite on the flotation of chalcopyrite in seawater. *Miner. Eng.* **2018**, *125*, 10–14. [[CrossRef](#)]
33. Chen, Z.; Ren, Z.; Gao, H.; Zheng, R.; Jin, Y.; Niu, C. Flotation studies of fluorite and barite with sodium petroleum sulfonate and sodium hexametaphosphate. *J. Mater. Res. Technol.* **2019**, *8*, 1267–1273. [[CrossRef](#)]
34. Li, Z.-H.; Han, Y.-X.; Li, Y.-J.; Gao, P. Effect of serpentine and sodium hexametaphosphate on ascharite flotation. *Trans. Nonferr. Met. Soc. China* **2017**, *27*, 1841–1848. [[CrossRef](#)]
35. Li, W.; Li, Y. Improved understanding of chalcopyrite flotation in seawater using sodium hexametaphosphate. *Miner. Eng.* **2019**, *134*, 269–274. [[CrossRef](#)]
36. Cumming, M.H.; Leonard, A.R.; Lecorre-Bordes, D.S.; Hofman, K. Intra-fibrillar citric acid crosslinking of marine collagen electrospun nanofibres. *Int. J. Biol. Macromol.* **2018**, *114*, 874–881. [[CrossRef](#)]
37. Nataraj, D.; Sakkara, S.; Meenakshi, H.N.; Reddy, N. Properties and applications of citric acid crosslinked banana fibre-wheat gluten films. *Ind. Crops Prod.* **2018**, *124*, 265–272. [[CrossRef](#)]

38. Galvão, A.C.; Robazza, W.S.; Arce, P.F.; Capello, C.; Hagemann, D.H. Experimental study and modeling of citric acid solubility in alcohol mixtures. *J. Food Eng.* **2018**, *237*, 96–102. [[CrossRef](#)]
39. Hao, H.; Li, L.; Yuan, Z.; Liu, J. Comparative effects of sodium silicate and citric acid on the dispersion and flotation of carbonate-bearing iron ore. *J. Mol. Liq.* **2018**, *271*, 16–23. [[CrossRef](#)]
40. Wei, Q.; Dong, L.; Jiao, F.; Qin, W. Use of citric acid and Fe(III) mixture as depressant in calcite flotation. *Colloids Surf. A Physicochem. Eng. Asp.* **2019**, *578*, 123579. [[CrossRef](#)]
41. Wang, Y.; Khoso, S.A.; Luo, X.; Tian, M. Understanding the depression mechanism of citric acid in sodium oleate flotation of Ca²⁺-activated quartz: Experimental and DFT study. *Miner. Eng.* **2019**, *140*, 105878. [[CrossRef](#)]
42. Liu, X.; Luo, H.; Cheng, R.; Li, C.; Zhang, J. Effect of citric acid and flotation performance of combined depressant on collophanite ore. *Miner. Eng.* **2017**, *109*, 162–168. [[CrossRef](#)]
43. Xia, L.; Hart, B. The role of citric acid in the flotation separation of rare earth from the silicates. *Miner. Eng.* **2015**, *74*, 123–129. [[CrossRef](#)]
44. Zeng, X.; Xu, L.; Tian, J.; Yin, W.; Yang, Y.; Deng, W. Effect of a CA depressant on flotation separation of celestite from fluorite and calcite using SDS as a collector. *Miner. Eng.* **2017**, *111*, 201–208. [[CrossRef](#)]
45. Zhu, H.; Qin, W.; Chen, C.; Chai, L.; Jiao, F.; Jia, W. Flotation separation of fluorite from calcite using polyaspartate as depressant. *Miner. Eng.* **2018**, *120*, 80–86. [[CrossRef](#)]
46. Abdalla, M.A.M.; Peng, H.; Younus, H.A.; Wu, D.; Abusin, L.; Shao, H. Effect of synthesized mustard soap on the scheelite surface during flotation. *Colloids Surf. A Physicochem. Eng. Asp.* **2018**, *548*, 108–116. [[CrossRef](#)]
47. Liu, X.; Huang, G.-Y.; Li, C.-X.; Cheng, R.-J. Depressive effect of oxalic acid on titanite during ilmenite flotation. *Miner. Eng.* **2015**, *79*, 62–67. [[CrossRef](#)]



© 2019 by the authors. Licensee MDPI, Basel, Switzerland. This article is an open access article distributed under the terms and conditions of the Creative Commons Attribution (CC BY) license (<http://creativecommons.org/licenses/by/4.0/>).